Title: An anomalous Wtb coupling at a linear collider

Author: Karol Kołodziej

Citation style: Kołodziej Karol. (2004). An anomalous Wtb coupling at a linear collider. "Physics Letters B" (Vol. 584, iss. 1-2 (2004), s. 89-97), doi 10.1016/j.physletb.2004.01.017

Available online at www.sciencedirect.com
SCIENCE DIRECT®
Physics Letters B 584 (2004) 89–97
PHYSICS LETTERS B
www.elsevier.com/locate/physletb

An anomalous Wtb coupling at a linear collider ☆

K. Kołodziej

Institute of Physics, University of Silesia, ul. Uniwersytecka 4, PL-40007 Katowice, Poland

Received 12 December 2003; accepted 10 January 2004

Editor: P.V. Landshoff

Abstract

Differential cross sections of secondary particles in a process of top quark pair production and decay into six fermions at a linear collider with an unpolarized and a longitudinally polarized electron beam are computed to the lowest order in the standard model and in the presence of an anomalous Wtb coupling. It is illustrated that the latter has a little impact on the differential cross sections. In particular, it is shown that the angular distribution of a secondary lepton receives practically no contribution from the anomalous Wtb coupling, even if the top quark is produced off shell and the non-double resonance background contributions are taken into account. This finding is in accordance with the decoupling theorem that has been proven in literature [Phys. Lett. B 476 (2000) 87; Phys. Lett. B 529 (2002) 82; Phys. Lett. B 557 (2003) 55; Pramana 54 (2000) 791, hep-ph/0002006] in the narrow top quark width approximation.

1. Introduction

Future high luminosity e^+e^- linear collider with its very clean experimental environment will be the most suitable tool for searching for the effects of physics beyond the standard model (SM). As the top quark is the heaviest matter particle ever observed, with mass close to the energy scale of the electroweak symmetry breaking, such non-standard effects may in particular manifest themselves in departures of the top quark properties and interactions from those predicted by SM. Needless to say, the discovery of such departures would give hints toward understanding physics beyond SM at higher energy scales. Therefore, measurements of the top quark properties and interactions, at the precision level of a few per mille, belong to the research program of any future e^+e^- linear collider [2].

At the linear collider, top quarks are produced in pairs in the process

$$e^+e^- \to t\bar{t}. \tag{1}$$

Due to a large decay width, t and $\bar{t}$ of reaction (1) almost immediately decay, predominantly through the following channels

$$t \to bW^+ \quad \text{and} \quad \bar{t} \to \bar{b}W^-, \tag{2}$$

with W^+ and W^- decaying into two fermions each. Thus, what one actually observes are reactions of the form

$$e^+e^- \to 6\text{f}, \tag{3}$$

☆ Work supported in part by the Polish State Committee for Scientific Research (KBN) under contract No. 2 P03B 045 23.
E-mail address: kolodzie@us.edu.pl (K. Kołodziej).

0370-2693
doi:10.1016/j.physletb.2004.01.017

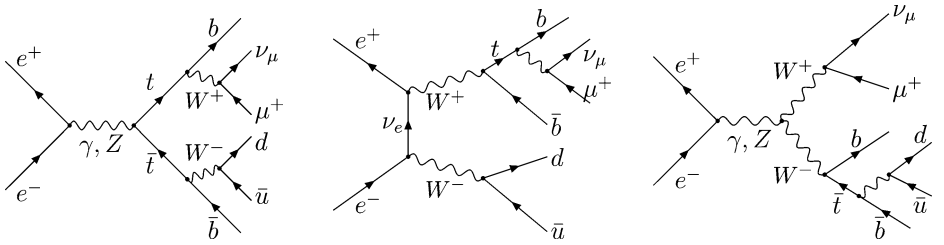

Fig. 1. Examples of the Feynman diagrams of reaction (9): (a) the double resonance 'signal', (b) and (c) the single resonance diagrams.

where 6f denotes a 6 fermion final state that is possible in SM. Any specific channel of (3) receives contributions typically from several hundred Feynman diagrams already at the lowest order of SM, whereas there are only two signal diagrams that contribute to it, for example, see Fig. 1(a).

Another interesting consequence of the very short life time of the top, $\tau_t = 1/\Gamma_t \approx 1/(1.5\ \mathrm{GeV})$, is that its spin can be directly observed. As the top quark decays before it hadronizes, information about its spin is passed directly to its decay products and can be best gained by measurement of the angular distribution of its decay products [3]. Therefore, it is interesting to look at an influence, which extensions of the pure left-handed Wtb coupling that governs decays (2) to the lowest order of SM, may have on some differential cross sections of (3). This issue has been already investigated in literature [1,4–6]. In [1], a decoupling theorem has been proven, which states that the angular distribution of the secondary lepton resulting from a decay of top quark produced in (1) receives no contribution from the anomalous Wtb coupling in the narrow top quark width approximation.

In the present Letter, the influence of the anomalous Wtb coupling on the process of top quark pair production and decay is analyzed numerically in a more realistic case, where the top quark pair is produced off shell and a complete set of the Feynman diagrams contributing to any specific channel of (3) at tree level is taken into account, including the non-double resonance background contributions. It is illustrated that the existence of anomalous form factors $f_2^{\pm}$ which assume values within present experimental limits has rather little an influence on differential cross sections of secondary particles of reaction (3). In particular, it is shown that the angular distribution of a secondary lepton of a semileptonic channel of (3) receives practically no contribution from the anomalous Wtb coupling, which is in accordance with the decoupling theorem quoted above.

2. An anomalous Wtb coupling

Departures of the Wtb coupling from SM can be best parametrized in terms of the effective Lagrangian [4]. The effective Lagrangian used in this Letter has been written down in Eq. (3) of [7]. The corresponding Feynman rules for the Wtb vertex are

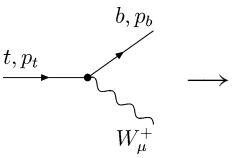

$$\Gamma^{\mu}_{t\to bW^+} = -\frac{g}{\sqrt{2}}V_{tb} \times \left[\gamma^{\mu}\left(f_1^- P_- + f_1^+ P_+\right) - i\sigma^{\mu\nu}(p_t - p_b)_{\nu} \times \left(f_2^- P_- + f_2^+ P_+\right)/m_W\right], \quad (4)$$

and

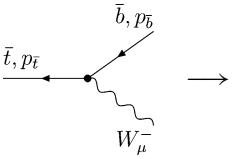

$$\Gamma^{\mu}_{\bar{t}\to\bar{b}W^-} = -\frac{g}{\sqrt{2}}V^*_{tb} \times \left[\gamma^{\mu}\left(\bar{f}_1^- P_- + \bar{f}_1^+ P_+\right) - i\sigma^{\mu\nu}(p_{\bar{t}} - p_{\bar{b}})_{\nu} \times \left(\bar{f}_2^- P_- + \bar{f}_2^+ P_+\right)/m_W\right]. \quad (5)$$

In Eqs. (4) and (5), V_{tb} is the element of the Cabibbo–Kobayashi–Maskawa (CKM) matrix, $P_\pm = (1 \pm \gamma_5)/2$ are chirality projectors, p_t ($p_{\bar{t}}$) is the four momentum of the incoming t ($\bar{t}$) and p_b ($p_{\bar{b}}$) is the four momentum of the outgoing b ($\bar{b}$); $f_i^\pm$ and $\bar{f}_i^\pm$, $i = 1, 2$ are the vertex form factors. If the Wtb interaction conserves $\mathcal{CP}$, which is assumed in the rest of the Letter, then the following relationships between the form factors of Eqs. (5) and (4) hold

$$\bar{f}_1^+ = f_1^+, \qquad \bar{f}_1^- = f_1^-, \quad \text{and}$$
$$\bar{f}_2^+ = f_2^-, \qquad \bar{f}_2^- = f_2^+. \tag{6}$$

The lowest order SM vertex is then reproduced by setting

$$f_1^- = 1, \qquad f_1^+ = f_2^- = f_2^+ = 0. \tag{7}$$

As the experimental value of $|V_{tb}|$ is 0.9990–0.9993 [8] and deviation of the (V + A) coupling f_1^+ from zero is severely constrained by the CLEO data on $b \to s\gamma$ [9], in the numerical analysis, the results of which are presented in the next section, $f_1^\pm$ are fixed at their SM values of Eq. (7), $V_{tb} = 1$ and modifications of the Wtb vertex by non-zero values of the other two anomalous form factors, f_2^+ and f_2^-, which are often referred to as the magnetic type anomalous couplings, are considered. Typical values of $f_2^\pm$ are [10]

$$\left| f_2^\pm \right| \sim \frac{\sqrt{m_b m_t}}{v} \sim 0.1. \tag{8}$$

They contradict neither the unitarity limit obtained from the $t\bar{t}$ scattering at the TeV energy scale that gives the constraint $|f_2^\pm| \leqslant 0.6$ [11], nor the limits that are expected from the upgraded Tevatron, which are of order 0.2.

The matrix elements corresponding to Eqs. (4) and (5) have been programmed with the helicity amplitude method of [12,13] and then implemented into `eett6f`, a Monte Carlo program for top quark pair production and decay into 6 fermions at linear colliders [14].

3. Numerical results

In this section, numerical results for some differential cross sections of a selected semileptonic channel of (3) at the centre of mass system (CMS) energies typical for the future linear collider with an unpolarized and a longitudinally polarized electron beam are shown. The results obtained in the lowest order of SM are compared to those obtained in the presence of the anomalous Wtb coupling of Eqs. (4)–(6). To be more specific, let us consider the angular and energy distribution of a μ^+ and b-quark of the following reaction

$$e^+e^- \to b\nu_\mu \mu^+ \bar{b} d\bar{u}. \tag{9}$$

To the lowest order of SM, in the unitary gauge and neglecting the Higgs boson coupling to fermion lighter than b-quark, reaction (9) receives contributions from 264 Feynman diagrams, typical examples of which are depicted in Fig. 1.

The SM electroweak physical parameters used in the computation performed with `eett6f` are the following [8]:

$$m_W = 80.419\ \text{GeV}, \qquad \Gamma_W = 2.12\ \text{GeV},$$
$$m_Z = 91.1882\ \text{GeV}, \qquad \Gamma_Z = 2.4952\ \text{GeV},$$
$$G_\mu = 1.16639 \times 10^{-5}\ \text{GeV}^{-2},$$
$$m_e = 0.510998902\ \text{MeV},$$
$$m_\mu = 105.658357\ \text{MeV},$$
$$m_u = 5\ \text{MeV}, \qquad m_d = 9\ \text{MeV},$$
$$m_t = 174.3\ \text{GeV}, \qquad m_b = 4.4\ \text{GeV}. \tag{10}$$

The Higgs boson mass and width are assumed to be $m_H = 170$ GeV and $\Gamma_H = 0.3835$ GeV.

The SM electroweak coupling constants are given in terms of the electric charge $e_W = (4\pi\alpha_W)^{1/2}$ and electroweak mixing parameter $\sin^2\theta_W$ with

$$\alpha_W = \sqrt{2} G_\mu m_W^2 \sin^2\theta_W/\pi,$$
$$\sin^2\theta_W = 1 - m_W^2/m_Z^2, \tag{11}$$

where m_W and m_Z are physical masses of the $W^\pm$ and Z^0 boson specified in Eq. (10). The strong coupling constant is given by $g_s = (4\pi\alpha_s(M_Z))^{1/2}$, with $\alpha_s(M_Z) = 0.1181$. The CKM mixing is neglected. Using $\sin^2\theta_W$ of Eq. (11) together with the following substitutions

$$M_V^2 = m_V^2 - i m_V \Gamma_V, \qquad V = W, Z,$$
$$M_H^2 = m_H^2 - i m_H \Gamma_H, \qquad M_t = m_t - i\Gamma_t/2, \tag{12}$$

which replace masses in the corresponding propagators, both in the s- and t-channel Feynman diagrams, is in `eett6f` referred to as the '*fixed width scheme*'.

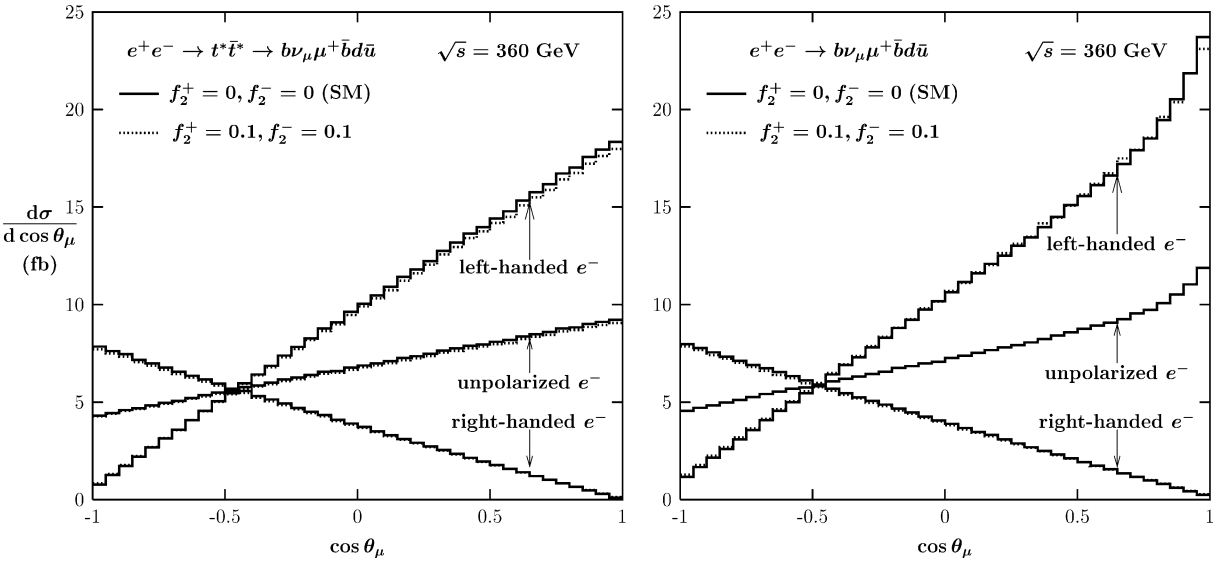

Fig. 2. The differential cross section $d\sigma/d\cos\theta_\mu$ of reaction (9) at $\sqrt{s} = 360$ GeV as a function of cosine of the μ^+ angle with respect to the initial e^+ beam. The figure on the left and right shows the double resonance approximation and the complete lowest order result, respectively.

The top quark width that is used in Eq. (12) is calculated to the lowest order taking into account the modified Wtb coupling and performing numerical integration over the 3 particle phase space. Assuming $\mathcal{CP}$ conservation that leads to relationships (6), the Wtb couplings of Eq. (4) and Eq. (5) result in the same value, within the MC error, for the width of the top and antitop.

Computations have been performed for different combinations of $f_2^+ = 0, \pm 0.1$, $f_2^- = 0, \pm 0.1$, assuming $f_1^- = 1$, $f_1^+ = 0$ and relationships (6). In the following only the results for $f_2^+ = f_2^- = 0.1$ are plotted, which show the biggest deviation from the SM predictions.

The results for angular and energy distributions of the μ^+ and b-quark of reaction (9) are presented in Figs. 2–9, where the plots on the right-hand side show results obtained with the complete set of the Feynman diagrams that contribute to (9) to the lowest order, while the plots on the left-hand side show results of the double resonance approximation that have been obtained by keeping the two 'signal' diagrams only, see Fig. 1(a), and neglecting all the other Feynman diagrams of reaction (9). In each of the figures, the solid histograms show the SM results, while the dotted histograms show the results in the presence of the anomalous Wtb coupling.

The differential cross section $d\sigma/d\cos\theta_\mu$ at $\sqrt{s} = 360$ GeV and $\sqrt{s} = 500$ GeV is plotted in Figs. 2 and 3, respectively, as a function of cosine of the μ^+ angle with respect to the initial e^+ beam. The different histograms have been obtained with an unpolarized and a longitudinally polarized electron beam. For the sake of simplicity, the level of longitudinal polarization is assumed to be 100%. Let us analyze the approximated 'signal' cross sections on the left-hand side of Figs. 2 and 3 first. The slant of the histograms representing unpolarized cross section caused solely by the Lorentz boost of the corresponding flat angular distribution of the μ^+ resulting from the decay of unpolarized top quark at rest. The slants of the histograms representing polarized cross sections at $\sqrt{s} = 360$ GeV, on the other hand, reflect proportionality of the angular distribution of μ^+ to $(1 + \cos\theta)$, if the spin of the decaying top-quark points in the positive direction of the z axis (spin up), and to $(1 - \cos\theta)$, if the spin of the decaying top-quark points in the negative direction of the z axis (spin down), see [15] for illustration. With the left-handedly (right-handedly) polarized electron beam that goes in the direction of negative z-axis, the top quark is produced preferably with its spin up (down). The corresponding $(1 \pm \cos\theta)$ behaviour of the μ^+ angular distribution is somewhat changed by the Lorentz boost, in particular at $\sqrt{s} = 500$ GeV.

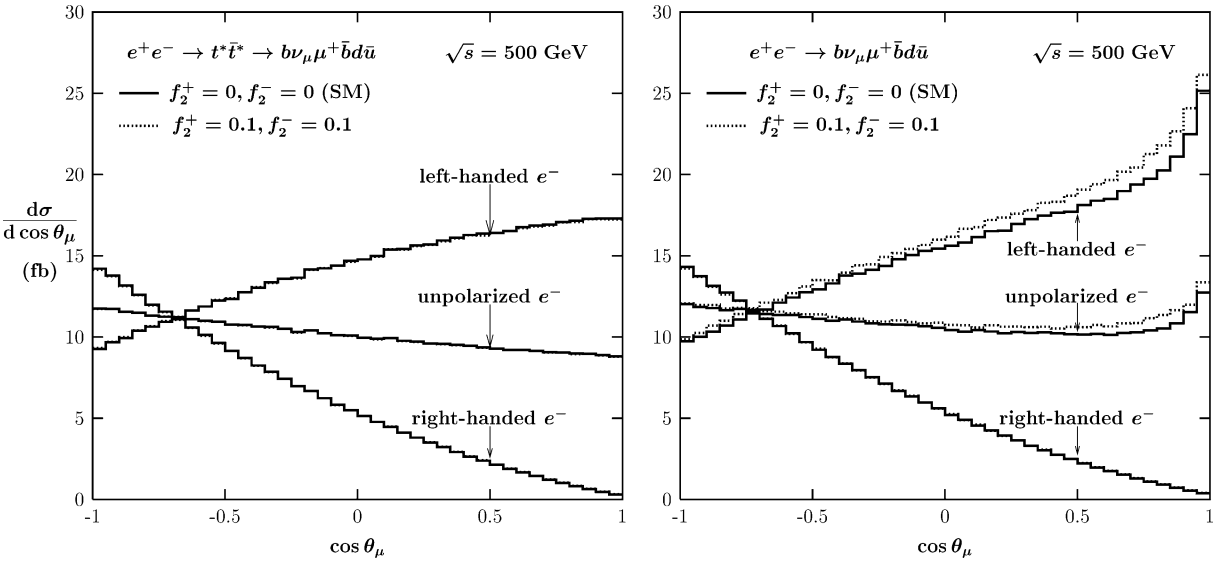

Fig. 3. The differential cross section $d\sigma/d\cos\theta_\mu$ of reaction (9) at $\sqrt{s} = 500$ GeV as a function of cosine of the μ^+ angle with respect to the initial e^+ beam. The figure on the left and right shows the double resonance approximation and the complete lowest order result, respectively.

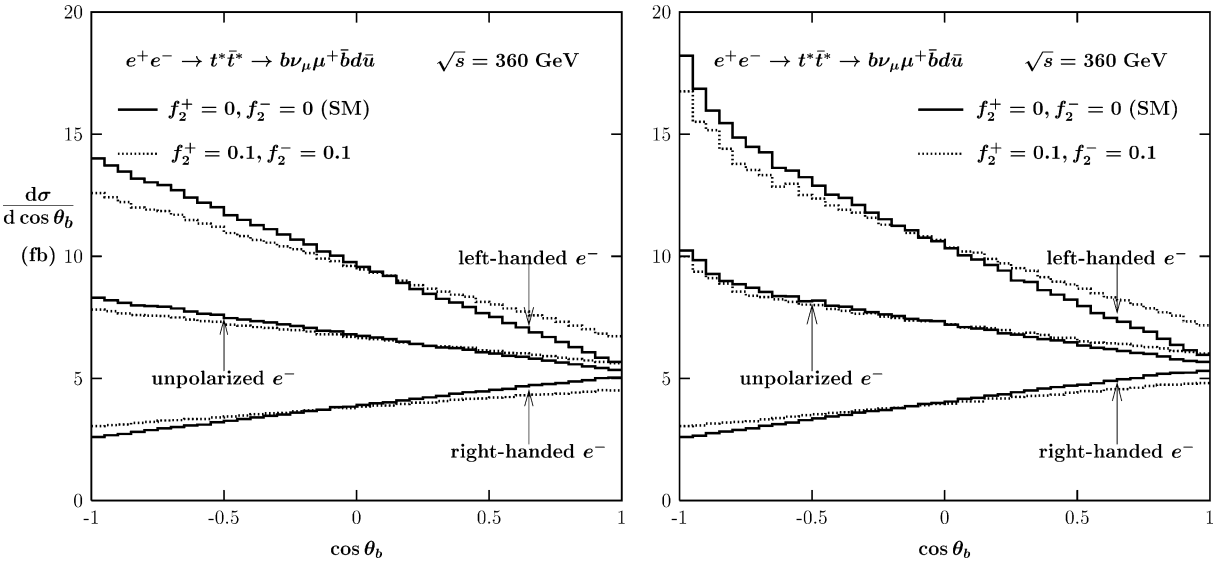

Fig. 4. The differential cross section $d\sigma/d\cos\theta_b$ of reaction (9) at $\sqrt{s} = 360$ GeV as a function of cosine of the b-quark angle with respect to the initial e^+ beam. The figure on the left and right shows the double resonance approximation and the complete lowest order result, respectively.

The dotted histograms represent the angular distribution of μ^+ in the presence of anomalous Wtb coupling (4)–(6) with $f_1^\pm$ set to their SM values, $f_1^+ = 0$, $f_1^- = 1$, and $f_2^+ = f_2^- = 0.1$. Except for a rather small effect in case of the left-handed electron beam at $\sqrt{s} = 360$ GeV, the change in the μ^+ angular distribution is hardly visible. This shows that the decoupling theorem of [1] holds in practice for reaction (9), even though the narrow top width approximation has not been applied here.

The corresponding histograms on the right-hand side of Figs. 2 and 3, which have been obtained with

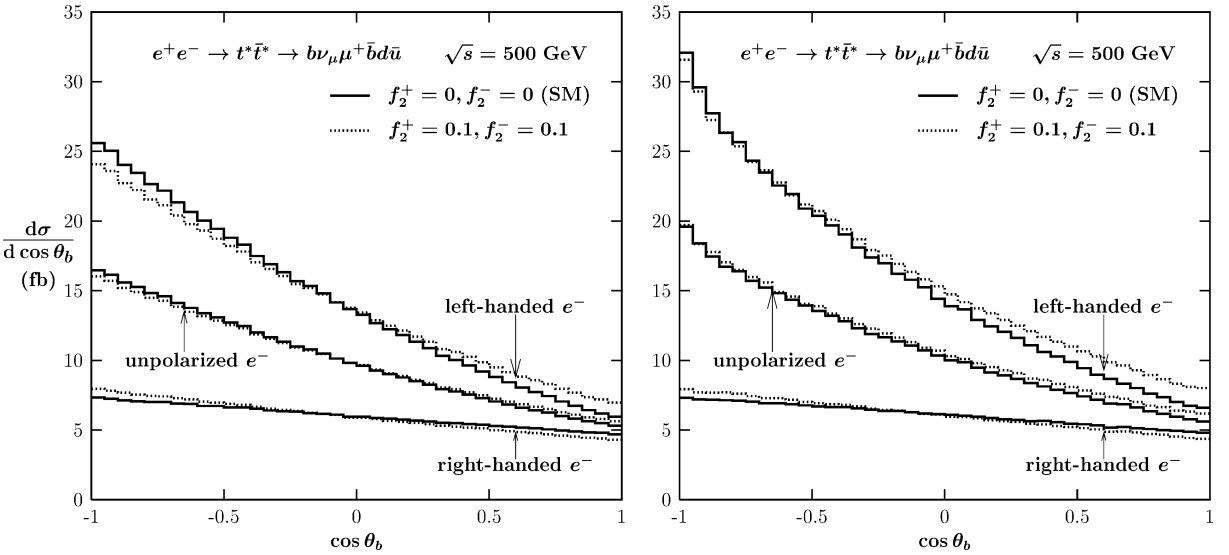

Fig. 5. The differential cross section $d\sigma/d\cos\theta_b$ of reaction (9) at $\sqrt{s} = 500$ GeV as a function of cosine of the b-quark angle with respect to the initial e^+ beam. The figure on the left and right shows the double resonance approximation and the complete lowest order result, respectively.

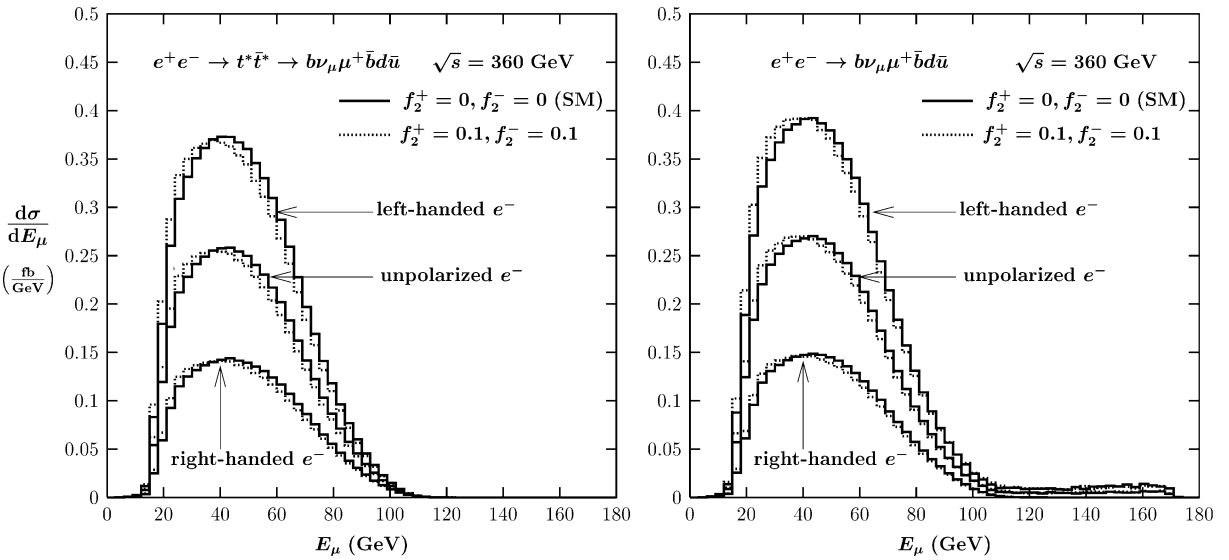

Fig. 6. The differential cross section $d\sigma/dE_\mu$ of reaction (9) at $\sqrt{s} = 360$ GeV as a function of the μ^+ energy in CMS. The figure on the left and right shows the double resonance approximation and the complete lowest order result, respectively.

the complete set of the Feynman diagrams of (9), show some distortions, that are caused by the non-doubly resonant background contributions. However, they essentially show similar angular dependence as the histograms on the left. It is interesting to note that the background enhances the anomalous effects at $\sqrt{s} = 500$ GeV, see the right-hand side of Fig. 3. This means that due to the non-resonance background the decoupling of the anomalous Wtb coupling does not work so perfect any more.

The corresponding angular cross sections for the b-quark $d\sigma/d\cos\theta_b$ at $\sqrt{s} = 360$ GeV and $\sqrt{s} =$

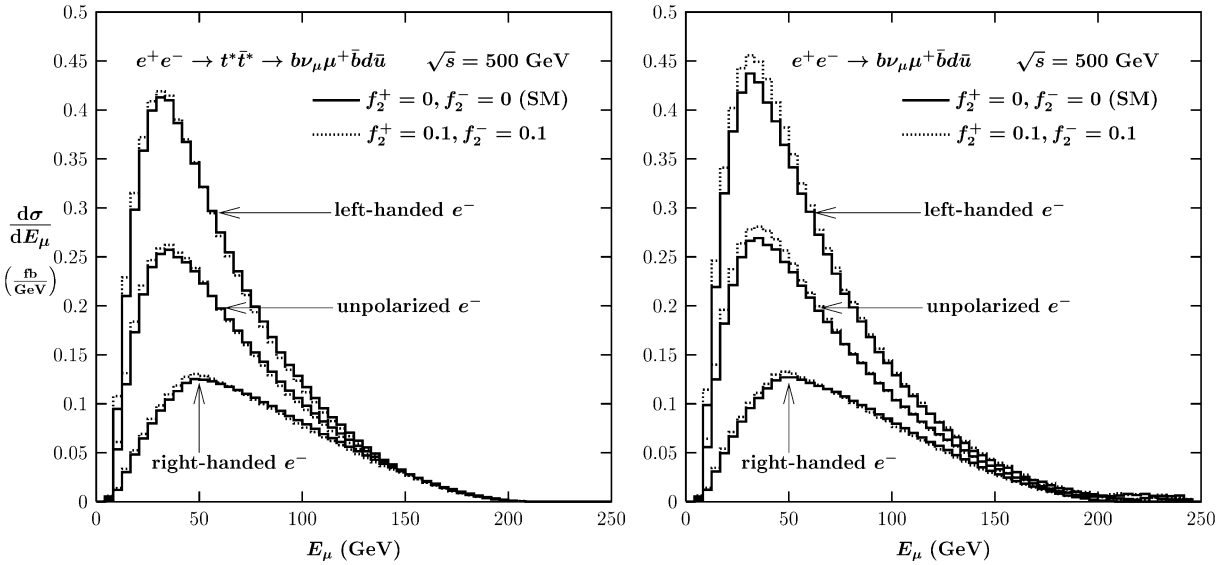

Fig. 7. The differential cross section $d\sigma/dE_\mu$ of reaction (9) at $\sqrt{s} = 500$ GeV as a function of the μ^+ energy in CMS. The figure on the left and right shows the double resonance approximation and the complete lowest order result, respectively.

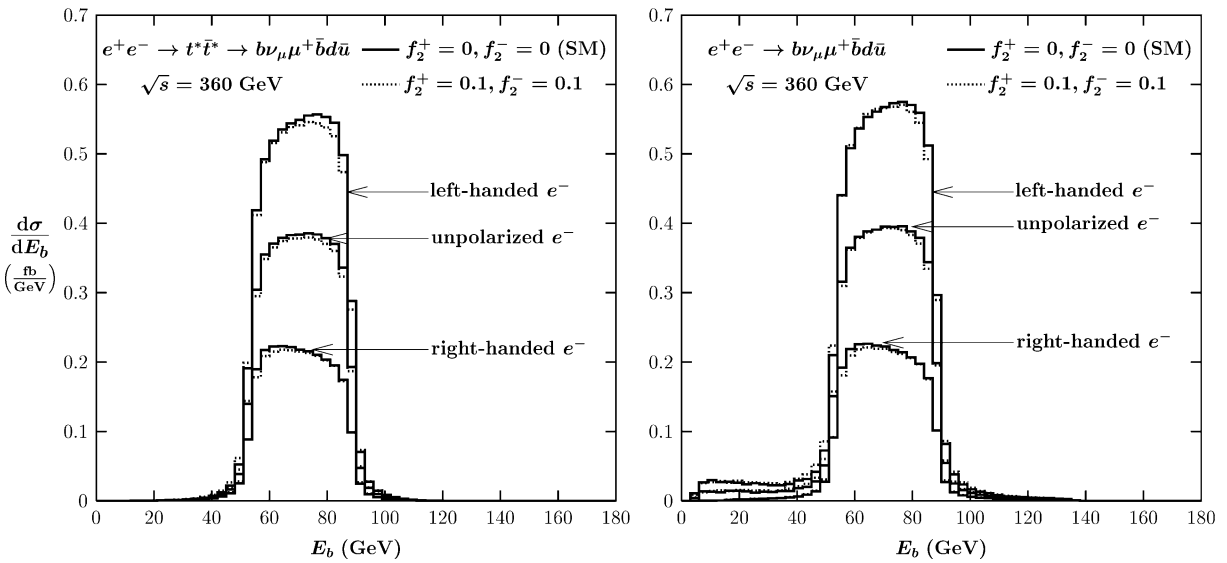

Fig. 8. The differential cross section $d\sigma/dE_b$ of reaction (9) at $\sqrt{s} = 360$ GeV as a function of the b-quark energy in CMS. The figure on the left and right shows the double resonance approximation and the complete lowest order result, respectively.

500 GeV are plotted in Figs. 4 and 5, respectively, as functions of cosine of the b-quark angle with respect to the initial e^+ beam. Again the dotted histograms represent the cross sections in the presence of the anomalous Wtb coupling (4)–(6) with $f_1^\pm$ set to their SM values, $f_1^+ = 0$, $f_1^- = 1$, and $f_2^+ = f_2^- = 0.1$. The numerical effect of the anomalous coupling is bigger than in Figs. 2 and 3. It is visible in particular for the longitudinally polarized electron beams.

The differential cross section $d\sigma/dE_\mu$ of reaction (9) at $\sqrt{s} = 360$ GeV and $\sqrt{s} = 500$ GeV is plotted in Figs. 6 and 7, respectively, as a function of the μ^+

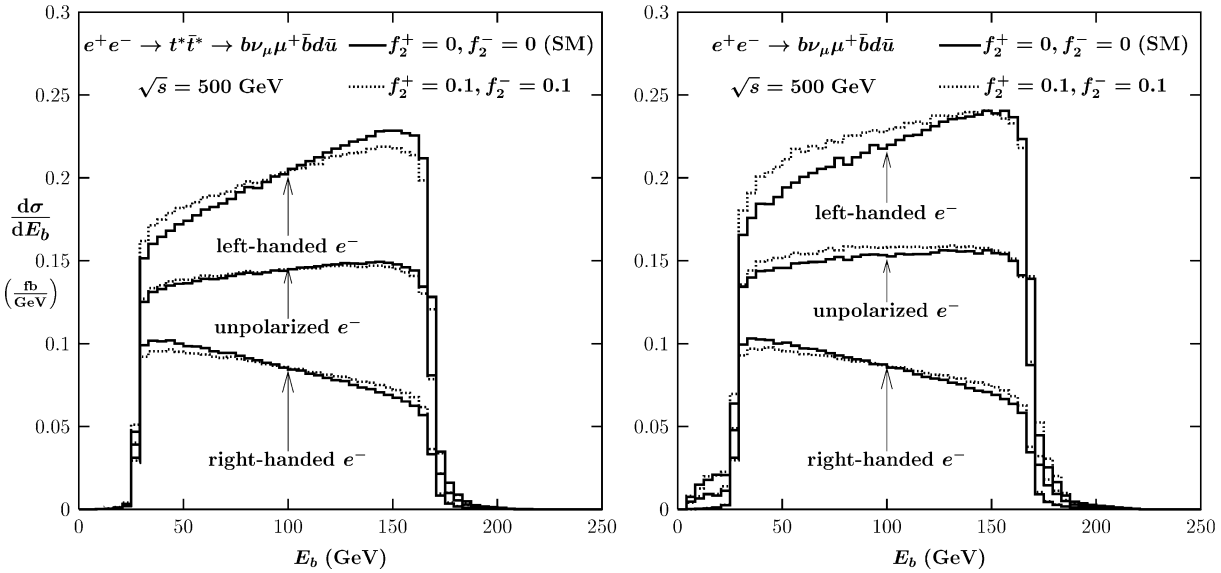

Fig. 9. The differential cross section $d\sigma/dE_b$ of reaction (9) at $\sqrt{s} = 500$ GeV as a function of the b-quark energy in CMS. The figure on the left and right shows the double resonance approximation and the complete lowest order result, respectively.

energy in CMS. Again the left and right figure show the double resonance approximation and the complete lowest order result, respectively. The corresponding cross sections $d\sigma/dE_b$ for the b-quark are plotted in Figs. 8 and 9. The anomalous effects in the energy distributions are bigger than in the angular distribution of μ^+. Note that they are not changed by the non-resonance background.

4. Summary

Results on angular and energy distributions of a μ^+ and b-quark of reaction (9), which is a typical semileptonic channel of the top quark pair production at a future linear collider, for the collisions of the unpolarized and longitudinally polarized electron beam against the unpolarized positron beam at $\sqrt{s} =$ 360 GeV and $\sqrt{s} = 500$ GeV, have been presented. The results, which have been computed to the lowest order in the SM and in the model with the anomalous Wtb coupling, taking into account the complete set of the lowest order Feynman diagrams of (9) and the two top quark pair production signal diagrams of Fig. 1(a) alone, illustrate how the anomalous Wtb coupling modifies the SM results. In particular, Figs. 2 and 3 illustrate that the angular distribution of μ^+ receives practically no contribution from the anomalous Wtb coupling. This shows that the decoupling theorem that has been proven in literature [1] in the narrow top quark width approximation holds in practice also in a more realistic case, where the top quark pair is produced off shell and the non-doubly resonant background contributions are taken into account. Analysis of the μ^+ distributions obtained with the longitudinally polarized beam shows that they are a very sensitive probe of the top quark polarization, as expected.

References

[1] B. Grządkowski, Z. Hioki, Phys. Lett. B 476 (2000) 87;
B. Grządkowski, Z. Hioki, Phys. Lett. B 529 (2002) 82;
B. Grządkowski, Z. Hioki, Phys. Lett. B 557 (2003) 55;
S.D. Rindani, Pramana 54 (2000) 791, hep-ph/0002006.

[2] R.-D. Heuer, D. Miller, F. Richard, P.M. Zerwas, et al., DESY 2001-011, ECFA 2001-209, hep-ph/0106315;
American Linear Collider Working Group Collaboration, T. Abe, et al., SLAC-R-570, Resource book for Snowmass, 2001;
ACFA Linear Collider Working Group Collaboration, K. Abe, et al., hep-ph/0109166.

[3] M. Jeżabek, J.H. Kühn, Nucl. Phys. B 320 (1989) 20.

[4] G.L. Kane, G.A. Ladinsky, C.-P. Yuan, Phys. Rev. D 45 (1992) 124.

[5] B. Grządkowski, Z. Hioki, Phys. Lett. B 476 (2000) 87, hep-ph/9911505;
E. Boos, M. Dubinin, M. Sachwitz, H.J. Schreiber, Eur. Phys. J. C 16 (2002) 471.
[6] K. Ciećkiewicz, K. Kołodziej, Acta Phys. Pol. B 34 (2003) 5497.
[7] K. Ciećkiewicz, K. Kołodziej, Acta Phys. Pol. B 32 (2001) 3797.
[8] K. Hagiwara, et al., Phys. Rev. D 66 (2002) 010001.
[9] CLEO Collaboration, M.S. Alam, et al., Phys. Rev. Lett. 74 (1995) 2885;
F. Larios, M.A. Perez, C.-P. Yuan, Phys. Lett. B 457 (1999) 334.
[10] R.D. Peccei, X. Zhang, Nucl. Phys. B 337 (1990) 269;
R.D. Peccei, S. Peris, X. Zhang, Nucl. Phys. B 349 (1991) 305.
[11] G.J. Gounaris, F.M. Renard, C. Verzegnassi, Phys. Rev. D 52 (1995) 451.
[12] K. Kołodziej, M. Zrałek, Phys. Rev. D 43 (1991) 3619.
[13] F. Jegerlehner, K. Kołodziej, Eur. Phys. J. C 12 (2000) 77.
[14] K. Kołodziej, Comput. Phys. Commun. 151 (2003) 339.
[15] K. Kołodziej, Acta Phys. Pol. B 34 (2003) 4511.